Fachtagung "Experimentelle Strömungsmechanik"
6. – 8. September 2016, Cottbus

Experimentelle Ermittlung momentaner Strömungsfelder – Einfluss von Wirbelstrukturen auf den Stofftransport an einer fixierten Einzelblase

Measurements of instantaneous flow structure – influence of vortical structures on mass transfer in vicinity of a fixed bubble

Sophie Rüttinger, Marko Hoffmann, Michael Schlüter
Hamburg Institute of Technology
Institute of Multiphase Flows
Eißendorfer Straße 38
21073 Hamburg

Momentane Strömungsfelder, Strömungsstruktur, Wirbelstrukturen, Stofftransport
Instantaneous flow fields, flow structure, vortical structures, mass transfer

Summary

The particular knowledge of mass transfer is of high interest for industrial processes in chemical, pharmaceutical, biological and food industry. To date, the mass transfer performance of apparatuses is mainly estimated by empirical Sherwood correlations, which take into account the flow regime with the Reynolds number of the bubble motion or with the turbulent kinetic energy dissipation rate (Lamont and Scott 1970). The dependence of flow structure on mass transfer processes has not been exhaustively researched yet.
As a result of the rapid development of (spatial and temporal) high resolution image based measurement techniques, the detailed acquisition of both flow and concentration fields has become possible. The processing of a magnitude of instantaneous data allows a deeper insight into transport processes.
In all engineering flows, vortices are present, and there are various reasons for their formation. They arise from turbulence, wakes, secondary flows and moving of fluidic interfaces. The understanding of processes in multiphase reactors and apparatuses can be enhanced by investigating the influence of the flow topology and thus, of vortex generation, evolution, interaction and decay (Kolar 2007), on mass transfer processes.
In this work, a brief overview is given over how vortical structures can be identified in measurement data and how they can be characterized in terms of their mass transfer relevance. Furthermore, experimental results with high spatial and temporal resolution are shown, illustrating the flow pattern and mass transfer in the vicinity of a single bubble at different flow conditions (different Reynolds numbers, artificial upstream wakes, etc.). Hydrodynamics are investigated by conducting high-speed Particle Image Velocimetry, the mass transfer coefficient is determined from the shrinking rate of a CO_2 bubble in water (Kastens et al. 2015) by conducting high-speed videography.

Introduction

In the past years and decades, a large body of work has been achieved concerning bubble column reactors, stirred vessels and other apparatuses which are used in industrial two phase processes. It is well known that a turbulent flow regime enhances transport of momentum, heat and mass. Due to fluctuation of velocity components and pressure,

Karlsruhe, Germany, ISBN 978-3-9816764-2-6

additional convective processes occur. But besides the impact of turbulence, also the impact of vortical structures on transport processes is thought to play an important role, see Figure 1. O'Reilly Meehan et al. (2016) investigated vortices within bubble wakes. They found that these vortexes cause relevant motions of the bulk fluid with the effect of local heat transfer enhancement. It suggests itself to also investigate the influence of vortexes on mass transfer and to find a model for description of these processes.

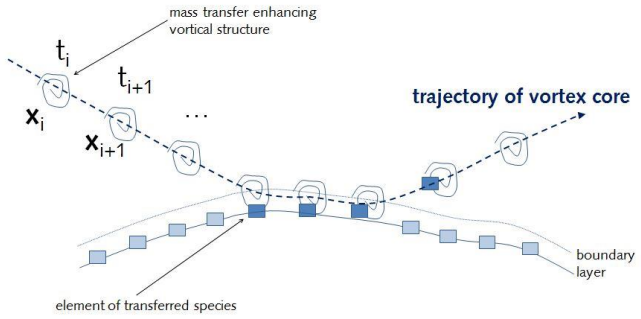

Figure 1: Schematic outline of mass transport by vortical structures.

Vortex identification

Before the impact of vortices on transfer processes can be analysed and discussed, a definition of *vortex* might be useful. Unfortunately, a definition accepted commonly does not exist and the demarcation to the term *coherent structure* is not sharp. While the definition given by Kline and Robinson (1989) and Robinson et al. (1989) and cited by Adrian et al. (2000) ask for a circular or spiral pattern of instantaneous streamlines, Jeong and Hussain (1995) show that this definition is not strict enough and additionally, they recognize that only statements concerning the core of the vortex can be made since the vortex size depends on the threshold chosen. Although Chong et al. (1990) think that 'it is unlikely that any definition of a vortex will win universal acceptance', their suggestion that 'a vortex core is a region of space where the vorticity is sufficiently strong to cause the rate-of-strain tensor to be dominated by the rotation tensor' is still the central assumption of most vortex identification criteria. Generally speaking, most of the vortex identification methods used base on the analysis of the velocity gradient tensor $\nabla \boldsymbol{u}$, which is divided into a symmetric $\boldsymbol{S}$ (rate-of-strain tensor) and an antisymmetric part $\boldsymbol{\Omega}$ (rotation tensor):

$$\nabla \boldsymbol{u} = \frac{1}{2}[(\nabla \boldsymbol{u}) + (\nabla \boldsymbol{u})^{\boldsymbol{T}}] + \frac{1}{2}[(\nabla \boldsymbol{u}) - (\nabla \boldsymbol{u})^{\boldsymbol{T}}] = \boldsymbol{S} + \boldsymbol{\Omega}$$

According to Chong et al. (1990), an eigenvalue problem is solved, as a vortex core is assumed to be at locations where $\nabla \boldsymbol{u}$ has complex eigenvalues. A more restrictive vortex identification scheme is the so-called Q criterion (Hunt et al. 1988). Q is the second invariant of $\nabla \boldsymbol{u}$ and depicts a local measure of the excess rotation rate relative to the strain rate (Chakraborty et al., 2005). According to the Q criterion, a vortex is a region with $Q > 0$, additionally, there must me a local pressure minimum. Since the local pressure minimum is not necessarily existent in $Q > 0$ regions, Jeong and Hussain (1995) suggest another criterion, which identifies local pressure minima. Starting with the Navier-Stokes equation for incompressible flows and neglecting unsteady irrotaional straining and viscous effects, they find that a vortex core is a connected region with two negative eigenvalues of $\boldsymbol{S^2} + \boldsymbol{\Omega^2}$. This condition is equivalent to the condition that after ordering the eigenvalues according size ($\lambda_1 \geq \lambda_2 \geq \lambda_3$), the second eigenvalue has to be negative: $\lambda_2 < 0$. For this reason, it is called

λ_2 criterion. A possibility to not only identify vortices, but also the strength and swirling plane is the swirling strength criterion (Zhou et al., 1999). It is based on the criterion of complex eigenvalues by Chong et al. (1990). Isoregions of the imaginary part of the complex eigenvalue pair of $\nabla \boldsymbol{u}$ can then be used to identify and also visualize vortices.
In planar flows, complex eigenvalue analysis, Q criterion and λ_2 criterion yield equivalent regions for vortices. Of course, for a very precise analysis of flow topology, a 3D domain has to be investigated. The vortex identification methods introduced here are suitable for 2D and 3D flow fields; in the former case, $\nabla \boldsymbol{u}$ is a 2x2 matrix, in the latter, a 3x3 matrix. 2D investigations bring the disadvantage that vortices will leave the field of view (which is a plane and not a volume) if their translational movement is not parallel to it. Therefore, the tracking of vortices can be difficult to treat.
While the most suggesting approach, the search for regions with high values of vorticity magnitude, is not expedient because 'vorticity cannot distinguish between pure shearing motions and the actual swirling motion of a vortex' (Kolar, 2007), Kolar (2007) suggests decomposing the velocity gradient tensor $\nabla \boldsymbol{u}$ not only into two, but into three parts: elongation, rigid-body rotation and shearing. Elongation and rigid-body rotation form the so-called residual tensor, from which vorticity is then calculated.
In this work, λ_2 criterion, Q criterion, total vorticity and residual vorticity are used. Often, vortices can be easily tracked by closed streamlines, which makes visualization comfortable.

Calculation of mass transfer coefficient from bubble shrinking rate

By observing the bubble volume over a certain period of time, the mass transfer coefficient can be derived (Kastens et al. 2015). Under the assumptions that a linear mass transfer balance can be used, that the CO_2 concentration in the water is negligible (water is stripped with N_2 gas to fulfil this condition), that CO_2 behaves approximately like an ideal gas and Henry's law can be used, the mass transfer coefficient k_L is determined as follows:

$$k_L = \frac{H(d_2^3 - d_1^3)}{(t_2 - t_1) d_{12}^2 C_V R T}$$

In this equation, H is the Henry constant, d_1, d_2 is the bubble diameter at time t_1, t_2, d_{12} is the arithmetic mean diameter of $d_1$and d_2, C_V is the molar concentration of water, R is the ideal gas constant and T is the temperature, which is held at 26°C during all the experiments, since above 25°C (and below 10 atm), the system CO_2-water can be assumed to be ideal (Houghton et al., 1957). The Sherwood number is then calculated by

$$Sh = \frac{k_L d_1}{D}$$

D depicts the diffusion coefficient of CO_2 in water.
For data validation, Sh-correlations are used as shown in Table 1.

Table 1: Sh-correlations used in this work

Flow regime	Sh-correlation	Reference
low Re, mobile interface	$Sh = 2 + 0.651 \frac{Pe^{1.72}}{1 + Pe^{1.22}}$	Brauer, 1971
low Re, rigid interface	$Sh = 2 + 0.333 \frac{Pe^{0.84}}{1 + Pe^{0.507}}$	Brauer, 1971
higher Re	$Sh = 0.991\, Pe^{1/3} \left(1 + \frac{Re}{4}\right)^{0.27}$	Clift et al., 1978

Experimental set-up and procedure

Experiments are conducted in a square duct made from acrylic glass with cross section 100 x 100 mm^2, for an overview, see Figure 2a. Entrance length is chosen to be at least 5 times the hydrodynamic diameter, i. e. 500 mm. An artificial upstream wake is generated by cylindrically shaped obstacles (d = 10 mm, 20 mm), which are placed at a distance of 55 mm and 110 mm to the bubble (from cylinder center to bubble center). As bulk fluid, deionized water is used which is continuously treated with N_2 gas to strip out CO_2. Temperature is held above 25°C, since below this value, the system CO_2 – water cannot be assumed to be ideal (Houghton et al. 1957). As seeding for PIV, PMMA particles (MicroParticles, 1-20 µm) coated with the fluorescent dye Rhodamine B (absorption at 530 nm, emission maximum at 607 nm) are used.

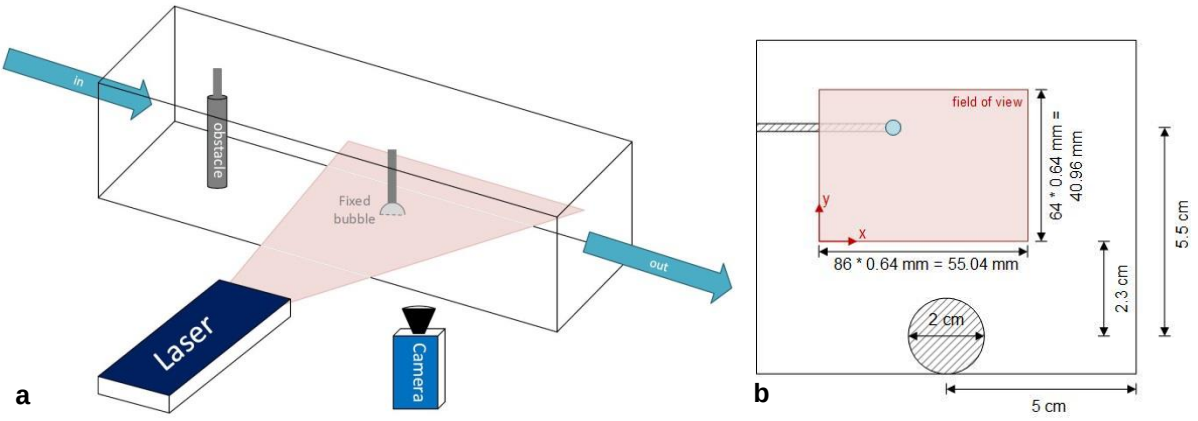

Figure 2: a) Experimental set-up (not to scale), b) Orientation guide: field of view within flow domain

The high-speed PIV system consists of a highspeed laser (Quantronix Darwin Duo Nd:YLF laser, 532 nm wavelength) which is run at 500 Hz and 50 µs pulse width, and a highspeed camera (PCO dimax HS2, 1400 x 1000 px, 12 bit CMOS) which is run at 500 fps and 100 µs exposure time, and equipped with a macro planar objective (Zeiss macro planar 2/50 mm, f-number: 2) and a bandpass filter, so that only the fluorescence light is recorded. The laser beam passes light sheet optics (rod lens, 50°) so that a horizontal laser light sheet (thickness approx. 1 mm) in vicinity of the bubble is produced. The high-speed camera is mounted perpendicular to the flow direction below the channel as it is outlined in Figure 2.

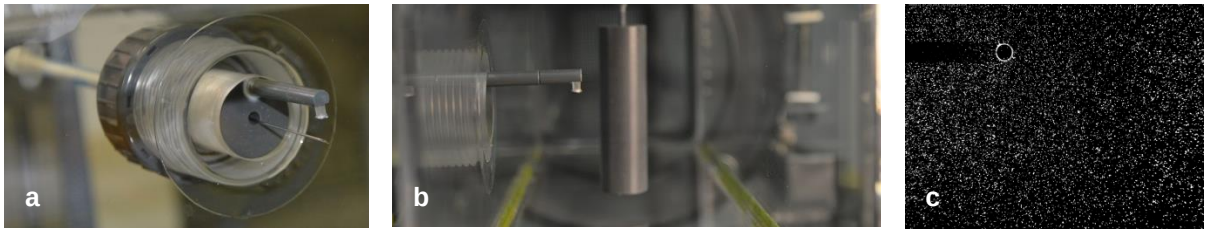

Figure 3: a) Generation and fixation of the single bubble, b) position of bubble and cylinder (view from the outlet), c) clearly visible bubble

The CO_2 bubble is produced using a syringe and a hollow needle brought into the duct through a septum. The bubble ascends into a cap which forces the bubble to adopt a nearly spheroidal shape (see Figure 3).
The bubble shrinking can be observed simultaneously with the PIV measurements as the bubble is clearly visible in the PIV image, see Figure 3c. 4 seconds after generation of the bubble, the PIV measurements are started. Bubble shrinking is observed from the beginning

of the recording until the ending after 16 seconds. From an ellipse which is positioned carefully at the inner bubble diameter, an equivalent bubble diameter is calculated.
PIV data processing is done using version 3.6.3 of PivView Software (PivTec GmbH). A window size of 32 x 32 px with 50% overlap fits best for the data. Target pictures yield the magnification factor, which is in this case 25 px/mm. Thus, the resultant spatial resolution is 0.64 mm. FFT correlation algorithm is chosen, which is applied using a multiple-pass interrogation with 3 iterations. As sub-pixel peak fit, least squares Gauss fit is chosen. Vectors with a pixel displacement of more than 1.5 times the average displacement are considered to be outliers and thus, other correlation peaks found in the correlation function are chosen or interpolation is performed.

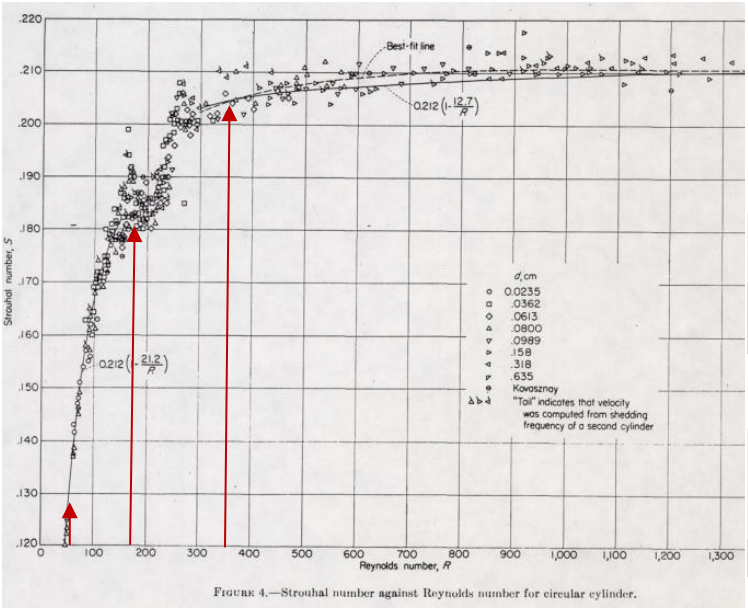

FIGURE 4.—Strouhal number against Reynolds number for circular cylinder.

$$Sr = \frac{f \cdot d_{cyl}}{u}$$

Re	Sr(Re)
50…150	$Sr = 0.212\left(1 - \frac{21.2}{Re}\right)$
300...2000	$Sr = 0.212\left(1 - \frac{12.7}{Re}\right)$

Re_{cyl}	Sr	f/ s^{-1}
34	0.08	0.024
67	0.14	0.021
180	0.19	0.304
358	0.20	0.16

Figure 4: Location of experimental parameters at the Roshko curve (Roshko, 1954)

Table 2 shows an overview over the experimental parameters. Using the curve by Roshko (1954), frequencies of vortex shedding can be estimated by the Strouhal number (see Figure 4).

Table 2: Experimental parameters

	no cylinder	cylinder d = 1 cm	cylinder d = 2 cm
Flow rate/ Lh^{-1} | overall velocity/ ms^{-1}	Re_{duct}	Re_{cyl}	Re_{cyl}
575 | 0.016	1792	180	358
100 | 0.003	334	34	67
0 | 0	0	0	0

Results and Discussion

In this work, it is possible to use the same recordings both for evaluation of mass transfer and hydrodynamics. Figure 5 shows the results of mass transfer calculations. The Sh number is plotted against the Pe number of the bubble. The graphs of the empirical correlations introduced in Table 1 are shown for data evaluation. The results are close to the empirical correlation for rigid interface which fits well to the fact that the bubbles are small

(approx. 3 mm) and that the cap prevents the major part of interface movement. An explanation for the visible fact that the Sh number is at higher Pe numbers even slightly lower than the empirical correlation curve for rigid interphase is that the cap prevents a part of the mass transfer. At the place where the bubble sticks to the cap, no CO_2 can be transferred into the fluid. The high Sh number at Pe=0 may show that even if no fluid flow is adjusted, there is still fluid motion. This can result from the heat of the laser light sheet (forced convection) or from the remaining tiny N_2 bubbles from the stripping process that educe fluid motion.
The cylinder with 2 cm diameter leads to slightly visible effects, whereas the smaller cylinder with 1 cm diameter does not significantly change the Sh number.

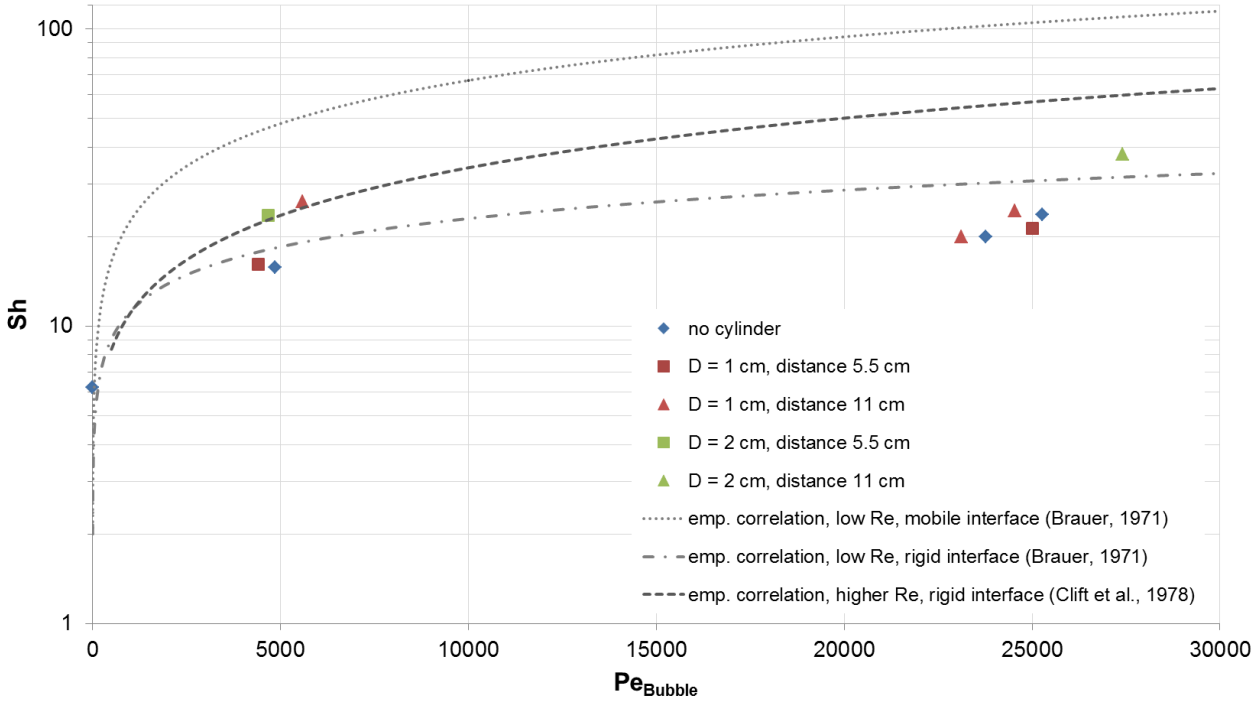

Figure 5: Global mass transfer results

While the global influence of the vortical structures induced by the cylinders is not observable, the investigation of the hydrodynamics shows significant local changes. For the highest cylinder Reynolds number in this work (Re_{cyl}=358) and distance between cylinder and bubble 5.5 cm, some visualisation images are shown. Here, the bubble, which is highlighted by a white circle, is positioned at the edge of the wake. Detailed information about the position of the viewing field within the flow domain is given in Figure 2b. The pink framings label vortical structures which are discussed in the following.
At time t_0, two vortical structures are visible in all vortex identification plots. One second later, at time t_1, the above structure is out of sight and the below structure has moved significantly. After 3 seconds at time t_3, the structure which was visible at t_0 and t_1 is gone and a new structure at nearly the same position as at t_1 is visible. From the calculations presented in Figure 4, a vortex shedding frequency of 0.16 was obtained for the case considered. Since the point of the vortex shedding (directly behind the cylinder) is not in the area of view (see Figure 2b) and the vortices might accelerate or decelerate after shedding, no statement can be made concerning the real vortex shedding frequency. But as it is pointed out exemplarily, the frequency of vortical structures occurring here is considerably higher than 0.16. This is plausible because of influence of walls and roughness, which cannot be neglected in this

experimental set-up. The values obtained from Figure 4 should therefore be understood as rough guides that display lower limits.
Already by observing the velocity vectors, vortical structures can be detected. The total vorticity magnitude (Figure 6b) (note that total vorticity as well as residual vorticity is plotted as a magnitude, since here, only regions of high magnitude are of interest) is very high at the transition from the wake to the accelerated area at the right and left hand area of the screen. This high vorticity magnitude results from shearing motion, since here, the area of very slow velocity directly behind the cylinder and the area of accelerated velocity above or below the cylinder come together. Also in the vicinity of the bubble, vorticity is high due to shear. This bothersome influence of shear is not visible any more at the residual vorticity plots (Figure 6c). Here, significantly fewer areas are yellow-coloured, which is a good achievement since only vortex cores – and no other activities of the fluid – are of interest. λ_2 (Figure 6d) and Q (Figure 6e) plots yield nearly the same results, although Q is less restrictive (since strictly speaking, also pressure has to be investigated: For a vortex core, there has to be a pressure minimum *and* Q > 0) and thus, the isoregions of Q > 0 are slightly larger than those of $\lambda_2 < 0$. Since the λ_2 criterion is a search for pressure minima, it is better suited for detection of vortices in this work. It is very interesting, that λ_2 as well as Q yield several low respectively high values in the regions where the comparison of total and residual vorticity shows high portion of shear. Therefore, the residual vorticity criterion might be even more restrictive than λ_2 criterion. Shearing motion close to interfaces will always be present (and can also be interesting for mass transfer considerations), but disturbs the vortex core detection. However, λ_2 minima are more distinctive and the plot shows less background noise. Therefore, a combination of λ_2 criterion and residual vorticity criterion is a good choice when investigating the influence of vortical structures on mass transfer.

Summary and outlook

In this work, global mass transfer experiments are conducted simultaneously with highspeed PIV experiments. From the shrinking rate of a CO_2 bubble in demineralized and N_2-stripped water, mass transfer coefficients and thus, Sherwood numbers are calculated and compared to different empirical correlations. Vortical structures produced by a cylindrically shaped obstacle do not show a significant influence in global mass transfer. The investigation of the hydrodynamics yield the result that vortices can be identified by all methods used, but residual vorticity and λ_2 criterion may deliver the best information.
In future work, a larger number of global mass transfer measurements will be performed to yield information about measuring errors and to recognize trends. Additionally, local concentration measurements are going to be conducted by using Laser Induced Fluorescence, so that the influence of vortical structures on local mass transfer can be observed.

Acknowledgements

The authors gratefully acknowledge the support which was given by the Deutsche Forschungsgemeinschaft (DFG) under grant No. SPP1740.
The first author wants to thank Sladana Crncevic, Malte Schonebohm and Katharina Törber.

Karlsruhe, Germany, ISBN 978-3-9816764-2-6

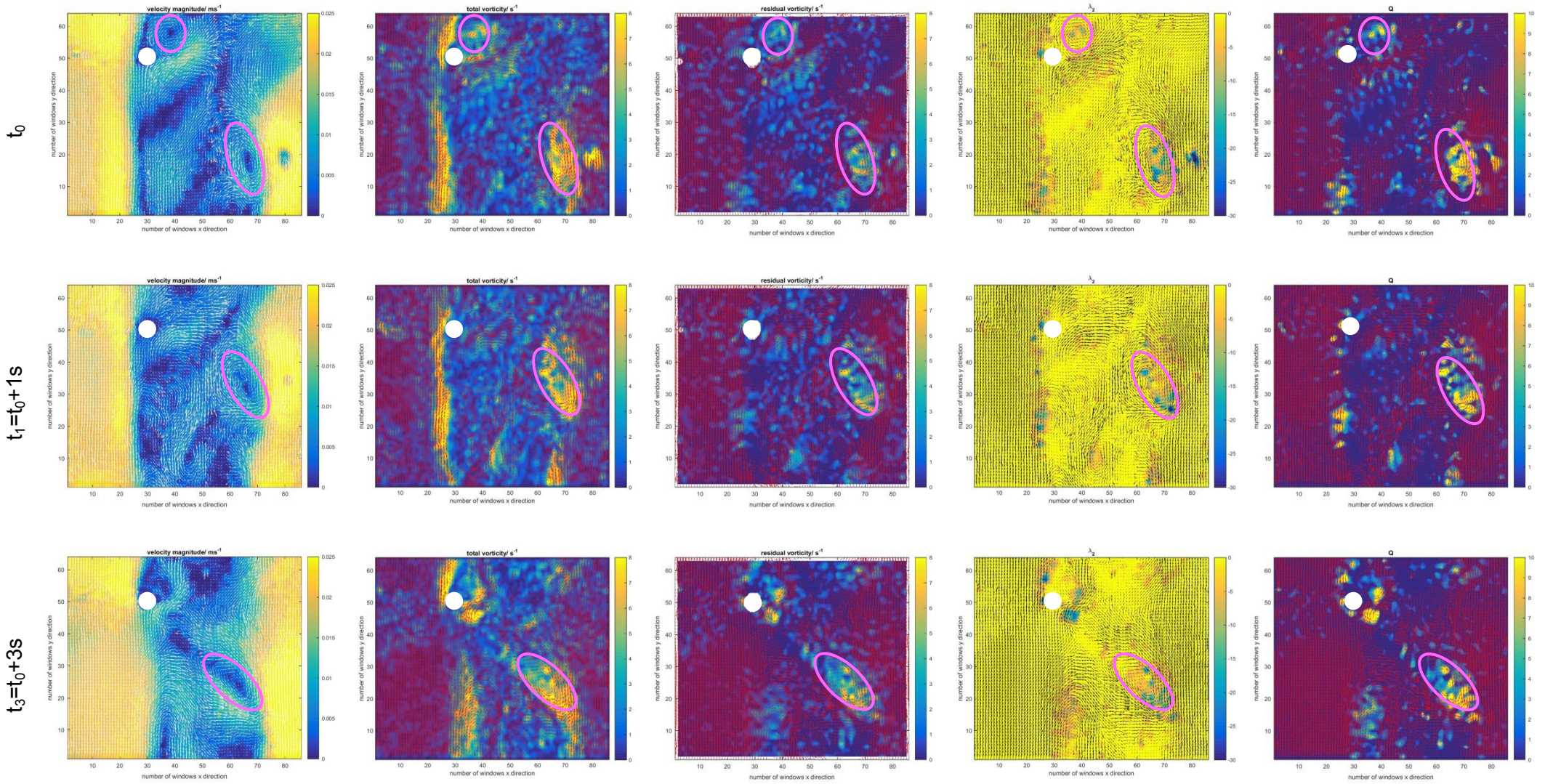

Figure 6: Results for the hydrodynamics of the Re_{cyl} = 358 flow case with distance between bubble and cylinder 5.5 cm. a) velocity field; b)-e) vortex identification methods

Literature

Adrian, R. J., Christensen, K. T., Liu, Z.-C., 2000: "Analysis and interpretation of instantaneous turbulent velocity fields", Experiments in Fluids, Vol. 29, pp. 275-290

Brauer, H., 1971: "Stoffaustausch einschließlich chemischer Reaktionen", Verlag Sauerländer AG, Aarau und Frankfurt am Main

Chakraborty, P., Balachandar, S., Adrian, R. J.,2005: "On the relationships between local vortex identification schemes", Journal of Fluid Mechanics, Vol. 535, pp. 189-214

Chong, M. S., Perry, A. E., Cantwell, B. J.,1990: "A general classification of three-dimensional flow fields", Physics of Fluids, Vol. 2, pp. 765-777

Clift, R., Grace, J. R., Weber, M. E., 1978: "Bubbles, drops, and particles", Dover publications, Inc., Mineola, New York

Houghton, G., McLean, A. M., Ritchie, P. D., 1957: "Compressibility, fugacity, and water-solubility of carbon dioxide in the region 0-36 atm. And 0-100°C", Chemical Engineering Science, Vol. 6, pp. 132-137

Hunt, J. C. R., Wray, A., Moin, P., 1988: "Eddies, stream, and convergence zones in turbulent flows", Center for Turbulence Research Report CTR-S88, pp. 193-208

Jeong, J., Hussain, F., 1995: "On the identification of a vortex", International Journal of Fluid Mechanics, Vol. 285, pp. 69-94

Kastens, S., Hosoda, S., Schlüter, M., Tomiyama, A., 2015: "Mass transfer from Single Taylor Bubbles in Minichannels", Chemical Engineering Technology, Vol. 38

Kolar, V., 2007: "Vortex identification: New requirements and limitations", International Journal of Heat and Fluid Flow, Vol. 28

Lamont, J. S., Scott, D. S., 1970: "An Eddy Cell Model of Mass Transfer into the Surface of a Turbulent Liquid", AiChE Journal, Vol. 16

O'Reilly Meehan, R., Donelly, B., Nolan, K., Persoons, T., Murray, D. B., 2016: "Flow structures and dynamics in the wakes of sliding bubbles", International Journal of Multiphase Flow, Vol. 84, pp. 145-154

Roshko, A., 1954: "On the development of turbulent wakes from vortex streets", National Advisory Committee for Aeronautics Report 1191

Houghton, G., McLean, A. M., Ritchie, P. D., 1957: "Compressibility, fugacity, and water-solubility of carbon-dioxide in the region 0-36 atm and 0-100°C", Chemical Engineering Science, Vol. 6, pp. 182-187

Zhou, J., Adrian, R. J., Balachandar, S., Kendall, T. M., 1999: "Mechanisms for generating coherent packets of hairpin vortices in channel flow", Journal of Fluid Mechanics, Vol. 387, pp. 353-396

Karlsruhe, Germany, ISBN 978-3-9816764-2-6